Revalidation of insular *Drymaeus* species from the southeastern Brazilian coast and implications for the *D. papyraceus* complex (Gastropoda: Eupulmonata: Bulimulidae)

Luiz Ricardo L. Simone
Museu de Zoologia da Universidade de São Paulo
São Paulo, SP, BRAZIL
lrsimone@usp.br
lrlsimone@gmail.com
https://orcid.org/0000-0002-1397-9823

ABSTRACT

Three insular species of *Drymaeus*—*D. castilhensis*, *D. micropyrus*, and *D. currais*—recently synonymized with the continental *D. papyraceus*, are herein revalidated. This revalidation is based on an in-depth anatomical study of *D. papyraceus* from mainland areas adjacent to the studied islands, which revealed significant differences that support their status as distinct species. Beyond these taxonomic conclusions, the results demonstrate that the anatomical study of closely related taxa must be much more detailed to resolve their taxonomy. Furthermore, the current concept of *D. papyraceus* may encompass a complex of morphologically similar species.

Additional Keywords: Bulimulidae, biodiversity, comparative anatomy, taxonomic revision, land snail

INTRODUCTION

Recently, three insular endemic species of *Drymaeus* Albers, 1850—namely *Drymaeus castilhensis* and *D. micropyrus* both Simone and Amaral, 2018, and *D. currais* Simone, Belz and Grenet, 2020—were synonymized with the mainland species *D. papyraceus* (Mawe, 1823) (La Pasta and Oliveira, 2025).

These putative synonymies are based on an anatomical study of specimens of *D. papyraceus* collected from the Rio de Janeiro region (La Pasta and Oliveira, 2025). The authors consider the conchological and anatomical differences among the above-mentioned species, as outlined in their original descriptions, to be insufficient to support their recognition as distinct species. They argue that *D. papyraceus* is a widely distributed and highly variable species, and that its occurrence on remote oceanic islands can be explained by other factors, such as passive dispersal by birds (La Pasta and Oliveira, 2025: 379).

However, an analysis of the anatomical study and the arguments supporting the proposed synonymies indicates that they are not sufficiently detailed for such closely related species. The four aforementioned species are indeed closely related and may be regarded as forming part of the "*D. papyraceus* group," which comprises species characterized by relatively fragile shells, an elongated outline, a deflected peristome, and irregular axial linear spotting on the shell surface.

In groups of closely related species, anatomical differentiation must be sought in subtle structural details across all organ systems. When such features are consistently maintained within an isolated population and differ from those of other populations, they provide important evidence for taxonomic distinction. If the analyses are limited to anatomy at a superficial level, the investigation becomes biased, potentially leading to the artificial lumping of multiple species into a single taxon. Consequently, important anatomical information may be overlooked (Simone, 2007).

The present study provides a more detailed anatomical characterization of the continental *D. papyraceus*, at a level comparable to that available for the three insular species, in order to test whether they represent a single species or distinct taxa. Similarities and differences are thoroughly examined, leading to the taxonomic conclusion that the most plausible interpretation is to recognize all four entities as valid and distinct species.

The regional variations and wide distribution currently attributed to *D. papyraceus* may indicate that this nominal taxon actually encompasses a complex of morphologically similar species. To avoid this broader complication, the present study is restricted to samples from a defined geographic area, namely the Atlantic Rainforest of mainland regions adjacent to the originally studied islands, specifically the coastal region of São Paulo State. Although additional material is available from northeastern Brazil to Argentina, these samples are saved for future investigations. The examined São Paulo material possibly belongs to the same population as those from Rio de Janeiro State studied by La Pasta and Oliveira (2025), as they are congruent forested areas.

It is important to emphasize that this article does not aim to resolve the broader taxonomic issues concerning

the *D. papyraceus* group, which is part of an ongoing, large-scale project encompassing a wider geographic range. Accordingly, the present study focuses solely on reassessing the status and revalidation of the species mentioned above.

Another species synonymized by La Pasta and Oliveira (2025), for example, is *D. magus* (Wagner, 1827). This species has been recently reviewed elsewhere (Rosa et al., 2025) and will be additionally addressed in a separate study.

MATERIALS AND METHODS

A complete list of the examined material is provided following the descriptions, as is customary in taxonomic studies. The specimens were collected under duly authorized projects (SISBIO license no. 10560-5). Samples were fixed in 75% ethanol without prior relaxation.

Dissections were performed using standard techniques, with specimens immersed in ethanol and examined under a stereomicroscope. All drawings were prepared with the aid of a *camera lucida* and are generally based on multiple specimens. Photographs of all stages of the dissections were taken using a digital camera coupled to the microscope. The description provided herein is intended to complement that of La Pasta and Oliveira (2025), with a focus on previously overlooked details and diagnostically important features. This complementary information is essential to support the comparative analysis and the revalidation of the insular species. Scanning electron microscopy (SEM) examinations were conducted using a Zeiss scanning electron microscope at the Laboratory of Electron Microscopy of the Museum of Zoology of the University of São Paulo (MZSP). This institution also houses most of the comparative type material.

Anatomical abbreviations: ab, accessory albumen chamber; **ac**, albumen chamber; **ad**, albumen gland duct; **ag**, albumen gland; **an**, anus; **bc**, bursa copulatrix; **bd**, bursa copulatrix duct; **bg**, buccal ganglion; **ce**, cerebral ganglion; **co**, collar vessel; **cv**, pulmonary (efferent) vein; **da**, duct to anterior lobe of digestive gland; **dd**, duct to posterior lobe of digestive gland; **df**, dorsal folds of buccal mass; **dg**, digestive gland posterior lobe; **eh**, epiphallus; **eo**, spermoviduct; **es**, esophagus; **fo**, free oviduct; **fp**, genital pore; **ga**, genital appendix; **gm**, genital muscle; **go**, gonad; **hd**, hermaphrodite duct; **in**, intestine; **m1–m10**, extrinsic and intrinsic odontophore muscles; **lm**, left secondary columellar muscle; **ma**, mantle, **mb**, mantle border; **mf**, third mantle fold; **mj**, jaw and peribuccal muscles; **ml**, inner mantle fold; **mo**, mouth; **mt**, outer mantle fold; **nv**, nerve; **oc**, odontophore cartilages; **od**, odontophore; **ot**, ommatophore; **pe**, penis; **pg**, pedal gland; **pl**, pleural ganglia; **pm**, penis muscle; **pn**, pneumostome; **po**, penis inner loop; **pp**, pedal ganglia; **ps**, penis sheath; **pt**, prostate; **pu**, pulmonary cavity; **ra**, radula; **rd**, receptacle duct; **rm**, right secondary columellar muscle; **rs**, radular sac; **rt**, rectum; **sa**, salivary gland aperture; **sc**, subradular cartilage; **sd**, salivary gland duct; **se**, septum between odontophore and esophageal origin in buccal mass; **sg**, salivary gland; **sl**, sublingual organ; **sp**, spermoviduct inner longitudinal fold; **sr**, seminal receptacle; **st**, stomach; **tg**, integument; **to**, tissue on radular ribbon preceding radular exposed region in buccal cavity; **ua**, ureter aperture; **ug**, ureter gutter; **un**, union of mantle border with nuchal surface; **ur**, secondary ureter; **ut**, uterus; **vd**, vas deferens; **vg**, vagina; **vm**, visceral mass.

SYSTEMATICS

Drymaeus papyraceus (Mawe, 1823) (Figures 1–4, 5B)

For a synonymy list see La Pasta and Oliveira (2025: 369), excluding *Drymaeus castilhensis, D. micropyrus* and *D. currais*. With that caveat, the present concept of *D. papyraceus* actually may encompass a set of similarly shelled species, thus additional synonymized species may be revalidated in the future.

Diagnosis: Shell conical, width ~40% of length, aperture ample, weakly deflected. Color white-cream, mostly with strong axial, dark brown spots; peri-umbilical area lacking spots; specimens lacking spots unknown. Spire angle ~40°. Protoconch ~4% of total length. Sculpture of strong axial undulations. Suture shallow, almost level with remainder of whorl. Peristome profile angle ~10°; length ~45% of total length. Columellar muscle straddling 1.6 whorls. Secondary columellar muscles with 7 origins in left and 7 in right; with only left muscle connected to main columellar muscle. Secondary ureter almost entirely closed, except for ~1/5 of its length preceding pneumostome. Urinary gutter T-shaped, lacking fold. Anus external to pneumostome, opened directly outside. Lung vessels developed only in anterior 1/3. Intrinsic pair of odontophore muscles: **m1v** lateral located, **m1d** present, **m2** with 6 narrow insertions, **m4** with multiple insertions, **m5** only half covered by **m4**, **m7** originating parallel to **m6**, **m10** thick and wide. Sigmoid intestinal loop very ample. Radular sac exposed. Radular rachidian of similar width those of neighboring teeth; marginal teeth with 1 outer secondary cusp; ~70 lateral teeth. Jaw lacking middle constriction. Salivary ducts penetrating dorsal buccal mass wall close to their apertures. Aperture of salivary glands lateral in middle level of buccal cavity; as opened pores. Stomach bulged, duct to posterior lobe of digestive gland originating from adjacent esophagus; duct to anterior lobe originating from stomach. Seminal receptacle duct short. Genital carrefour appendix absent. Albumen chamber duct single, inserting perpendicular to spermoviduct. Albumen chamber as initial curve of spermoviduct. Accessory albumen chamber present. Prostate occupying ~1/6 of spermoviduct surface; fold protecting sperm groove in inferior region inferior tall, thin and simple. Penis slender and long, lacking clear

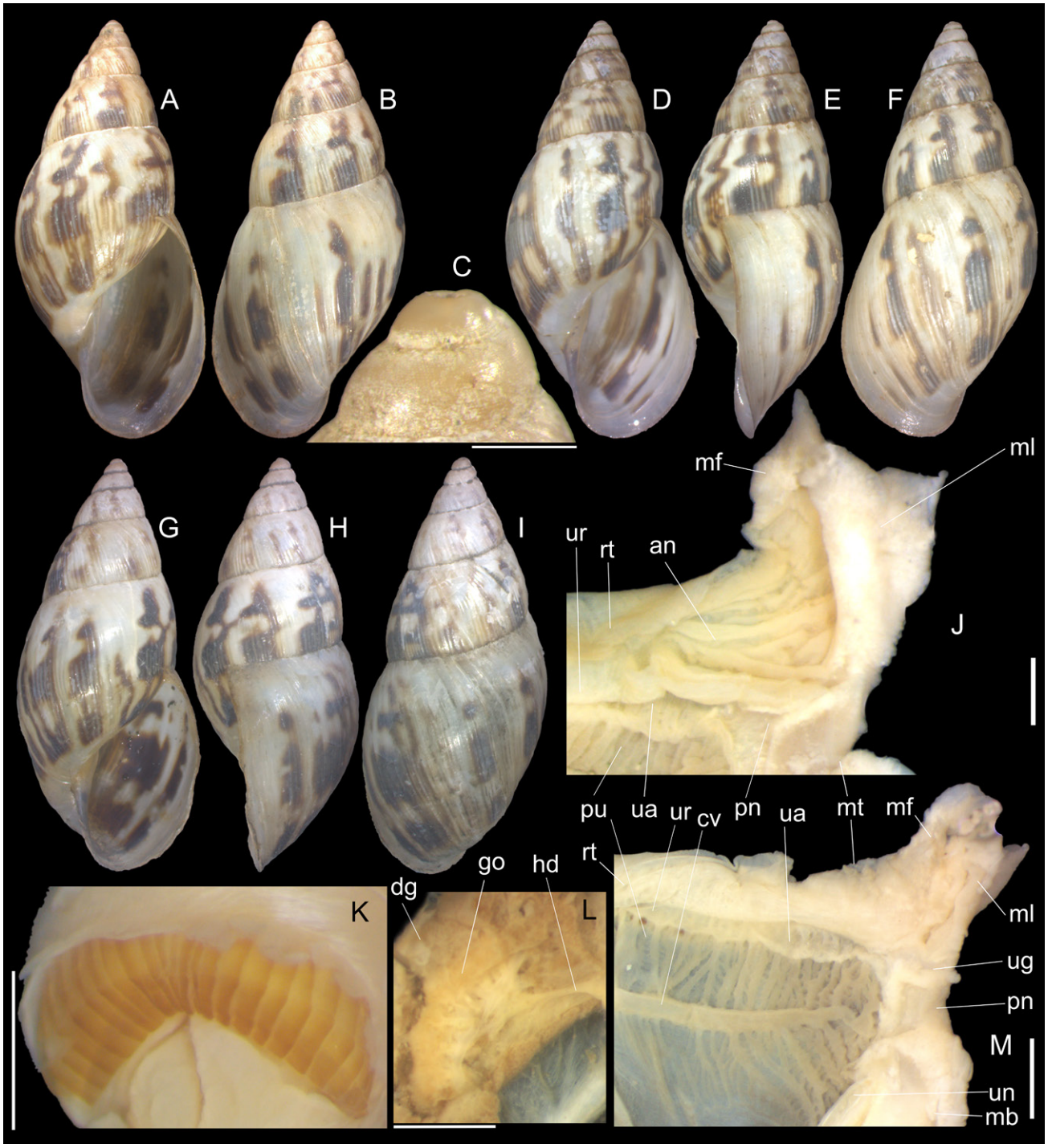

Figure 1. *Drymaeus papyraceus* photos of conchological and anatomical features. **A–C**. MZSP 90819 from Itariri, SP. **A**. Shell, apertural view (L 32.6 mm). **B**. Same, dorsal view. **C**. Apex in profile, scale= 1 mm. **D–F**. MZSP 168356 from Itanhaém, SP, apertural, right and dorsal views (L 31.8 mm). **G–I**. MZSP 158750 from Itanhaém, SP, apertural, right and dorsal views (L 31.8 mm). **J**. Pallial cavity, region of anus, inner lip of pneumostome sectioned and deflected upwards, anus and preceding rectal region opened longitudinally showing inner folds, scale bar= 1 mm. **K**. Jaw anterior plate in situ, anterior view, scale bar= 1 mm. **L**. Visceral mass, region of gonad, ventral view, scale bar= 2 mm. **M**. Pulmonary region close to pneumostome, ventral-inner view, inner lip of pneumostome sectioned and deflected upwards, scale bar= 2 mm.

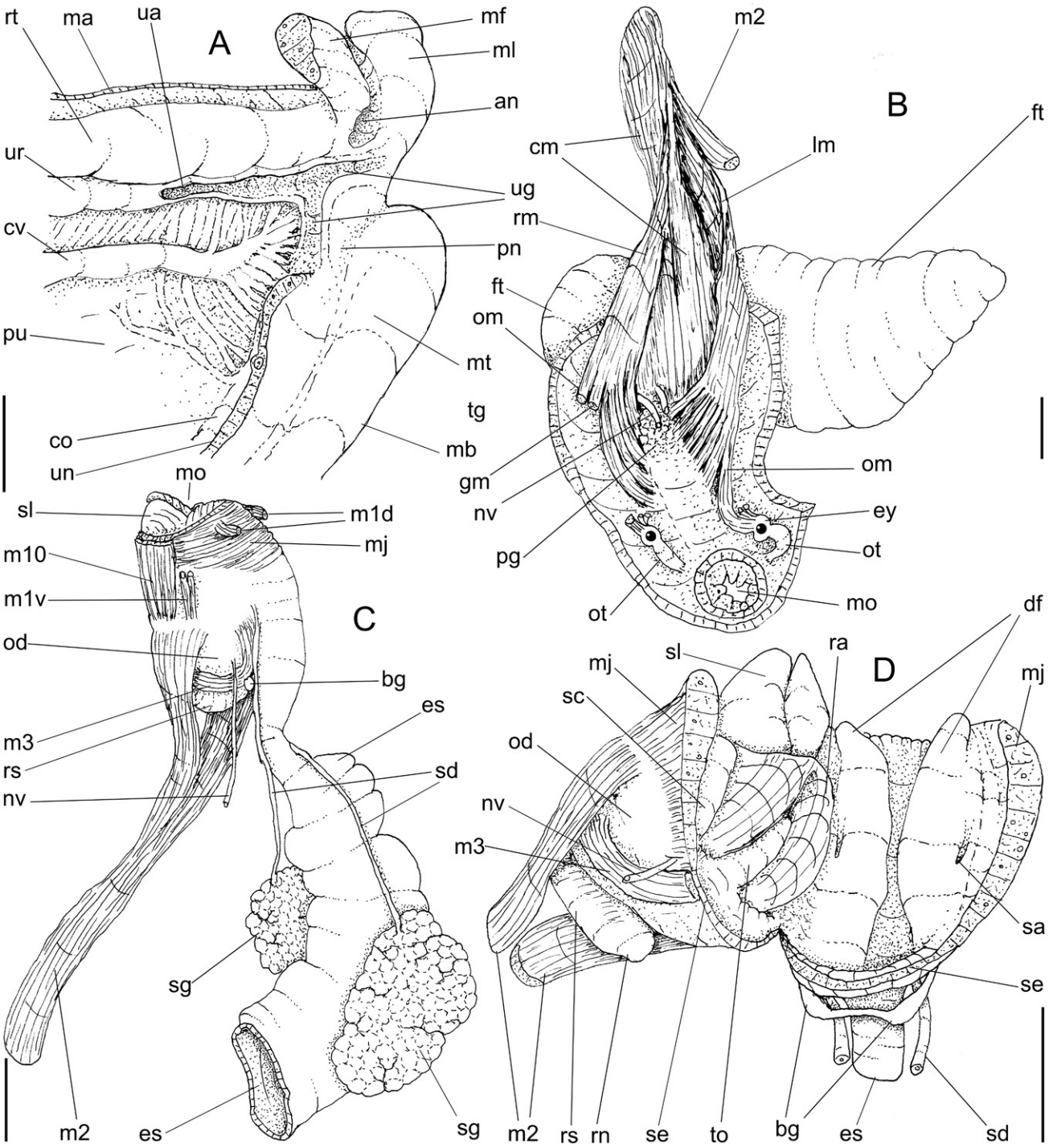

Figure 2. *Drymaeus papyraceus* anatomical drawings. **A**. Pulmonary region close to pneumostome, ventral-inner view, inner lip of pneumostome sectioned and deflected upwards. **B**. Head-foot, dorsal view; inner structures removed, integumentary and columellar muscles structures slightly expanded. **C**. Foregut, left view. **D**. Buccal mass, right view, buccal dorsal wall sectioned and deflected to right. Scale bars = 2 mm.

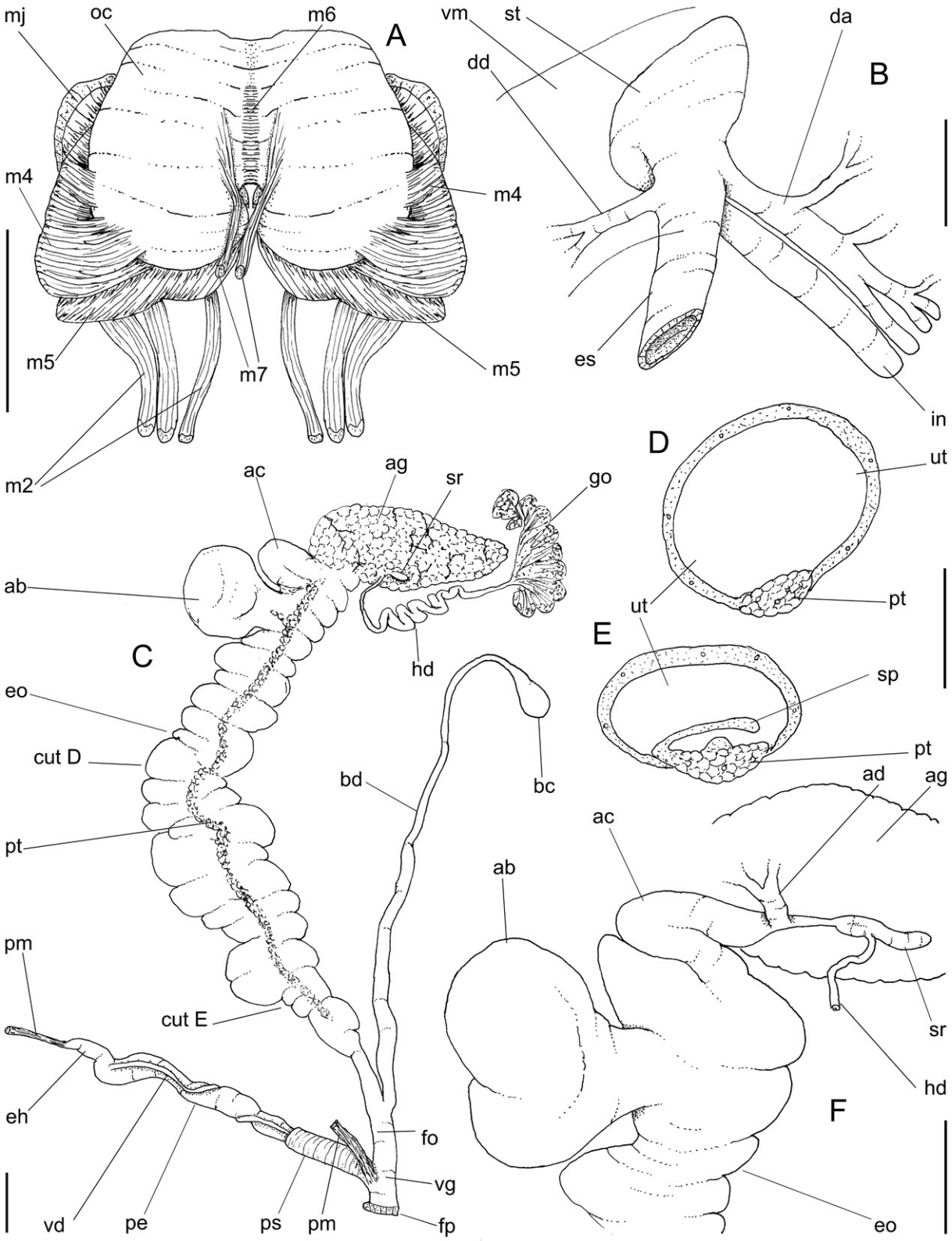

Figure 3. *Drymaeus papyraceus* anatomical drawings. **A**. Odontophore, dorsal view, superficial layer of muscles and structures removed, both cartilages deflected, radula removed, some main muscles also deflected. **B**. Midgut in situ, ventral view. **C**. Genital system, uncoiled, mostly dorsal view. **D–E**. Transverse sections in indicated regions (in C) of spermoviduct. **F**. Middle region of genital system, ventral view, some structures seen if albumen gland (ag) was transparent. Scale bars= 2 mm.

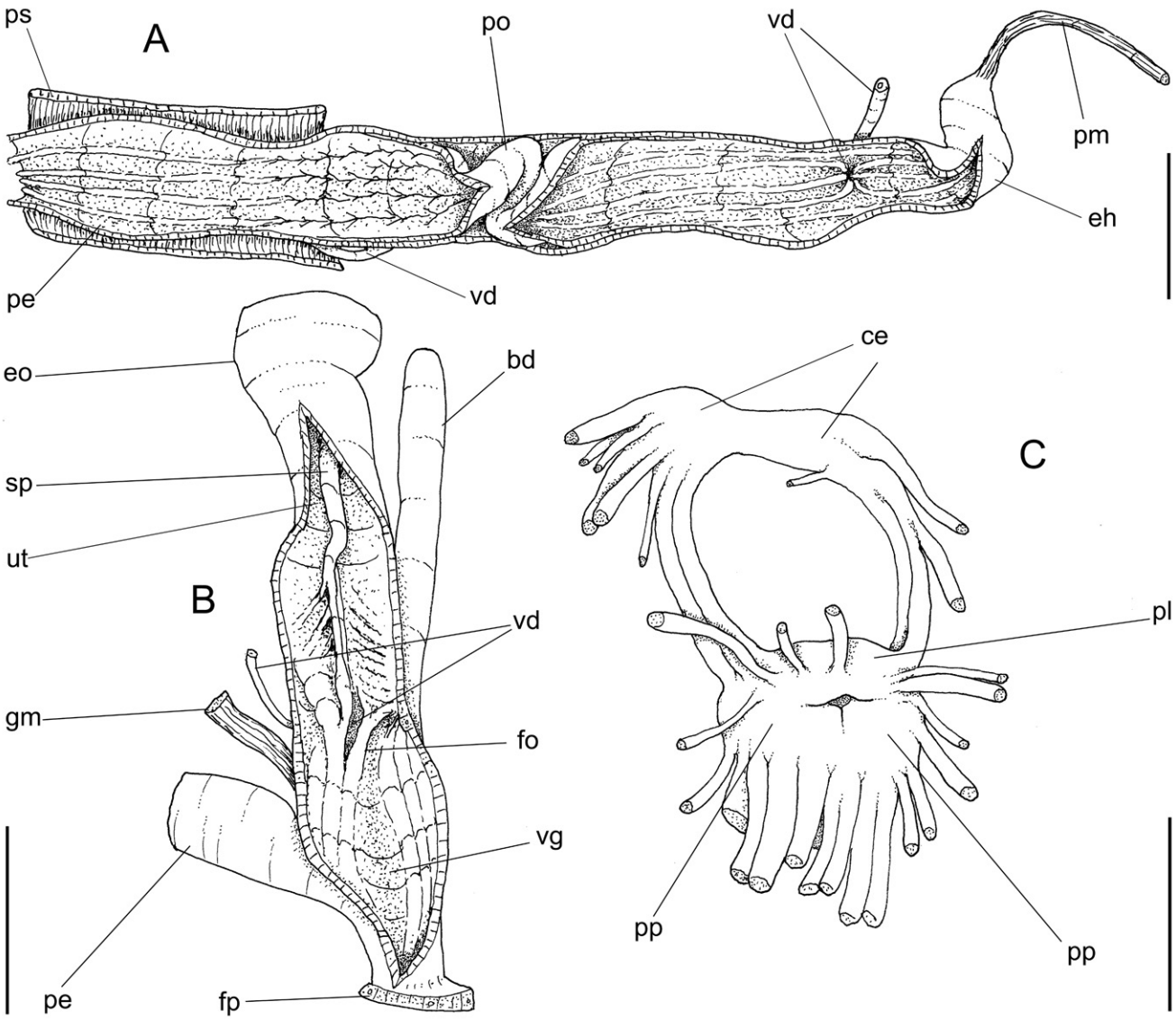

Figure 4. *Drymaeus papyraceus* anatomical drawings. **A**. Whole penis, opened longitudinally. **B**. Genital ducts, dorsal view, detail of its anterior region, some structures sectioned longitudinally. **C**. Central nervous system, dorsal view. Scale bars= 2 mm.

inner chambers; inner loop present in its middle region. Genital muscle present.

Description: Shell (Figures 1A–I): adult shell around 35 mm, conical-oval; apex bluntly acuminated; wider on last whorl; width ~40% shell length. Basal color pale-cream; pattern of brown to dark-brown spots arranged in irregular axial bands, barely forming narrow axial band with undulated proximal edge and irregular distal edge, forming 3 projections, central projections usually broader, reaching suture in spire region; pattern of each axial band slightly repetitive along successive whorls, sometimes coalescent (Figures 1E, G), sometimes with areas missing bands (Figures 1B, E, G); peri-umbilical area lacking spots (Figures 1A, D, G). Spire angle ~40°. Protoconch of 2 whorls, ~4% of total shell length, uniformly sculptured with delicate reticulate pattern (Figure 1C), with ~25 spiral lines in last whorl; transition to teleoconch well defined, slightly prosocline. Teleoconch smooth, except for strongly marked growth lines and even axial undulations, with ~5 whorls. Whorls profile weakly convex. Suture shallow, slightly oblique to columellar axis. Aperture prosocline (~10° from longitudinal general axis) (Figures 1E, H), oval; ~45% of shell length, ~60% of shell width. Peristome slightly reflected, especially on anterior region, partially covering umbilicus (Figures 1A, D, G). Body whorl ~65% shell length (Figures 1B, F, I). Umbilicus narrow. Other details in La Pasta and Oliveira (2025: 369).

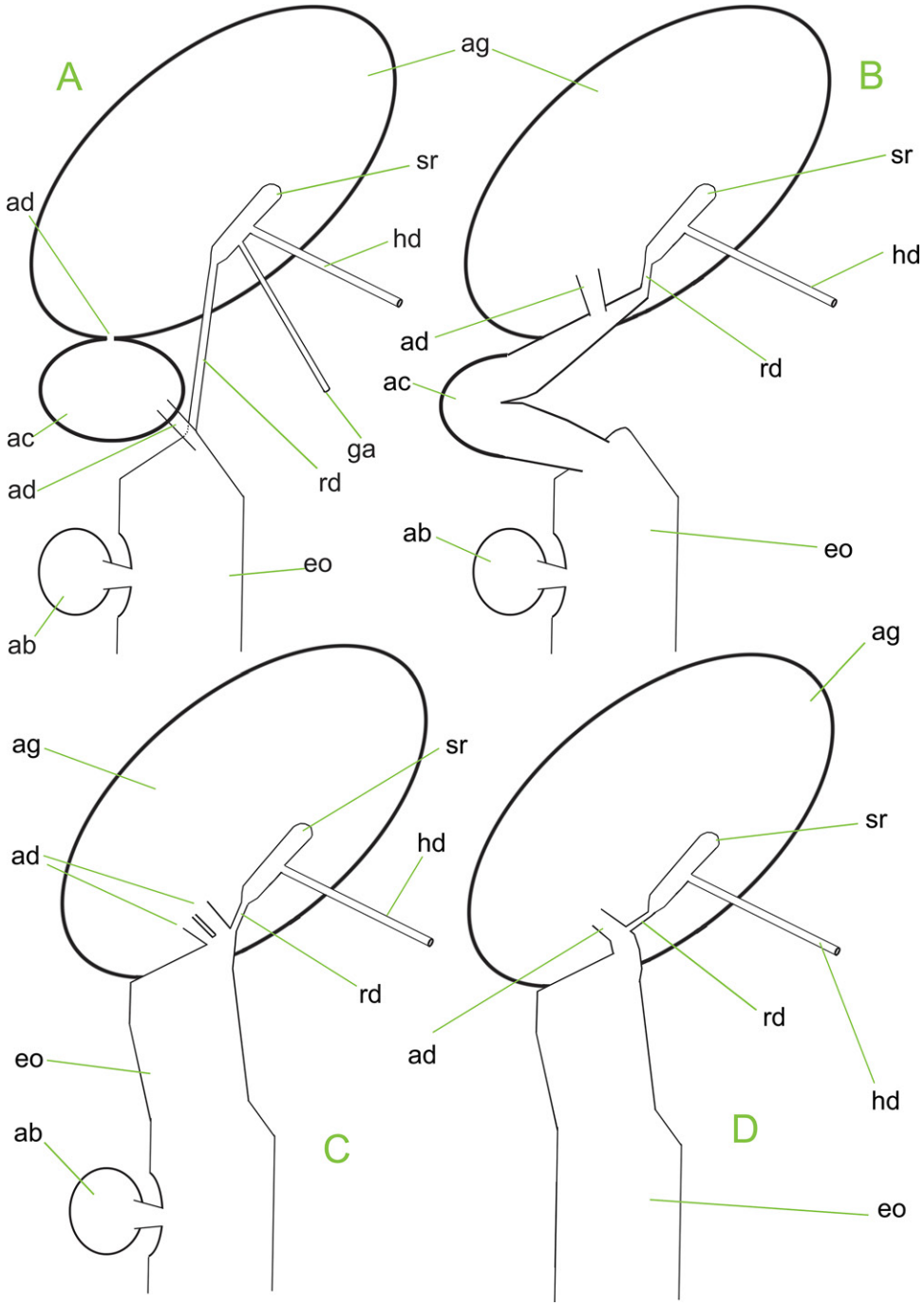

Figure 5. Schematic representation of carrefour (fertilization complex) and adjacent region of genital system of the 4 studied *Drymaeus* species, ventral view, showing structural differences. **A**. *D. currais*. **B**. *D. papyraceus*. **C**. *D. castilhensis*. **D**. *D. micropyrus*.

Head-foot (Figure 2B): of usual shape. Color uniformly clear. Columellar muscle thin, 1.6 whorls in length. Left secondary columellar muscle with 7 separated bundles in origin (Figure 2B: lm), and 4 in origin of right secondary columellar muscle (rm).

Mantle Cavity Organs (Figures 1J, M, 2A): Mantle border thick, lacking pigments. Pneumostome (**pn**) protected by ventral, right simple flap (**ml**), with ~1/5 of aperture length and additional small fold located in region of pneumostome (**mf**). Dorsal fold about double of ventral flap (mb), ~1.5 times longer. Pneumostome (**pn**) ~1/10 of aperture length, bearing air entrance, urinary escape (**ua**) in left-anterior side (**pn**), and anus in right-posterior side, separated by transverse fold (**an**). Urinary gutter anteriorly T-shaped (Figures 1M, 2A: **ug**),

with a branch flanking rectum-anus, another perpendicular, running mantle edge. Lung 1.5 whorls in length, twice as as wide. Pulmonary vessels clustered, sometimes bifurcating, conspicuous all along right side, mostly bearing transverse, rather perpendicular vessels; on left and right side of anterior third of pulmonary vein (**cv**), vessels visible only on anterior third, occupying approximately half right of this area, comprised of transverse vessels of similar aspect at right side, all of them connected to collar vessel (Figures 1M, 2A, **co**). Remaining regions of lung almost smooth, with imbricated vessels of difficult visualization. Pulmonary vein (cv) running longitudinally between middle and right thirds of pallial cavity roof, somewhat equidistant from rectum all along its length. Reno-pericardial area triangular, located posteriorly at middle level of posterior end, occupying ~25% of cavity length and ~70% of its width. Rectum (**rt**) and ureter (**ur**) narrow, running along right edge. Urinary aperture elongated (Figures 1M, 2A: **ua**), occupying ~1/10 of ureter length; its posterior end slightly rounded, its anterior end positioned just to the left of anus, T-shaped as described above.

Visceral mass: ~3.5 whorls in length. Similar in characters as other species, except for small and thin anterior lobe of digestive gland.

Circulatory and excretory systems: Similar to those described for related species.

Digestive system (Figures 2C, D, 3A, B): Arrangement of foregut essentially same as that described for *Drymaeus castilhensis* (Simone and Amaral, 2018: 171–172, figs. 41–44). Noteworthy features are: **m1v**, ventral pair of jugal muscle inserted more laterally positioned (Figure 2C); **m1a**, small pair of lateral jugal muscles absent; **m1d**, strong pair of buccal elevator jugal muscles, originated in dorsal inner wall of haemocoel, close to mouth, running towards ventral for short distance, inserting in each side of dorsal surface of mouth (Figure 2C); **m2**, pair of retractor muscles of buccal mass slightly narrower, with separated insertions in buccal mass, each one with 3 different origins (Figure 3A); **m3**, pair of superficial muscles running transversally along postero-lateral surface of buccal mass, from dorso-lateral region to region close to radular nucleus at m2 insertion; **m4**, with multiple origins along lateral edges of cartilages (Figure 3A); **m5**, pair of secondary dorsal tensor muscles of radula more medially located, ~half uncovered by m4 in its posterior region (Figure 3A); **m7**, originated in middle level of medial edge of cartilages (Figure 3A); **m10**, pair of ventral protractor muscles of buccal mass relatively thick; circular muscles of oral tube (mc) not so developed. Radular extending weakly beyond odontophore (Figure 2D). Jaw plate (Figure 1K) lacking medial slightly constriction, ~11–13 pairs of transverse folds medially narrow, gradually becoming wider towards lateral.

Radula: Approximately 1.5x longer than odontophore; with rachidian teeth and ~70 pairs of lateral teeth; no clear distinction between lateral and marginal teeth; all teeth with relative long and flattened base, located close to neighboring rows; central set of cusps rather small, located on anterior end of base. Rachidian tooth small, slightly smaller than neighboring teeth, ~1/100 of radular width; base ~3 times longer than wide, flattened, barely rectangular; central cusp with ~1/2 of base's size, tip blunt; pair of basal cusps with ~1/3 of central cusp's size. Lateral teeth similar to rachidian, except for being slightly larger, asymmetrical, arched towards lateral region; gradually weaker decreasing toward lateral teeth; set of cusps with ~1/2 of length of base; central cusp rounded pointed; medial cusps small, closer to central cusp tip; outer basal cusp ~half of central cusp in more central teeth, almost originating from base. Set of marginal teeth starting with no clear boundary from lateral teeth; marginal teeth shaped similarly to lateral teeth, except for having 4 similarly sized cusps, with some predominance of second cusp (check La Pasta and Oliveira, 2025: figs 12–14). Salivary glands covering esophagus in its region preceding its anterior 1/3 (Figure 2C: **sg**), forming two rounded, white, separated thin masses. Salivary ducts distinguishable on their anterior side, relatively broad, of ~1/10 anterior esophageal width (Figures 2C, D: **sd**). Salivary duct running along both sides of esophagus, running externally attached to dorsal buccal mass wall up to region of salivary aperture, penetrating buccal mass wall only in this region (Figure 2D: **sd**). Salivary ducts opening as longitudinal slit, on middle level of dorsal folds, on their lateral side (Figure 2D: **sa**). Esophagus 1 whorl long, with thin, mostly wide, flaccid walls lacking clear subdivisions (Figure 2C: **es**). Stomach (Figure 3B: **st**) blunt, curved, slightly bulged; gastric walls thin, flaccid; inner surface smooth. Esophageal insertion on posterior-left side (es), intestinal origin (**in**) dorsal to esophageal insertion, both close to columella. Duct to anterior lobe of digestive gland (**da**) originating from stomach, just anterior to esophageal insertion; highly branched, running adjacent to right intestine (Figure 3B: **in**). Duct to posterior lobe of digestive gland (**dd**) located on esophagus a short distance from esophageal insertion (Figure 3B: dd), slightly narrower than anterior duct. Intestine (in) ~half of width of esophageal insertion, all along its length, including narrow sigmoid loop in anterior lobe of digestive gland. Rectum and anus position described above (pallial cavity) (Figure 2A: **rt, an**). Anus sessile, as transverse slit on right end of mantle edge, directed externally, but still inside pneumostome (Figure 2A); inner surface with 7–8 longitudinal, uneven, simple folds (Figure 1J: **an**).

Genital System (Figures 1L, 3C–F, 4A, B): gonad, composed of ~8 lobes with minute digitiform acini (Figures 1L, 3C: **go**). Hermaphroditic duct (Figures 1L, 3C: **hd**) narrow and weakly coiled in both ends, gradually becoming very wider (up to 3x wider) and coiled in middle

half (Figure 3C: **hd**); inserting in middle level of left side of receptacle's edge (Figure 3F: **hd**). Seminal receptacle (Figures 3C, F: **sr**) relatively small, sac-like, ~4x longer than wide, with ~twice hermaphroditic duct width. Fertilization complex simple, located at narrow and elongated base of seminal receptacle (Figure 3F) as short duct of seminal receptacle (~1/3 of receptacle length). Genital appendix absent. Fertilization complex totally immersed in albumen gland (Figure 3C, 5B), inserting on posterior end of spermoviduct, albumen gland duct (Figure 3F: **ad**) relatively wide, simple, ~3x wider than receptacle's duct, inserted perpendicularly on its lateral surface. Albumen gland (Figure 3C: **ag**) solid, white, elliptical, 1.5x larger than gonad (~1/3 whorl). Duct of albumen gland subterminal, connected to distal end of receptable duct (Figure 3F: **ad**). Albumen chamber as differentiated initial curve of spermoviduct (Figures 3C, F: **ac**). Auxiliary albumen chamber (Figures 3C, F: **ab**) balloon-like, as wide as local spermoviduct, connected to it by narrow duct at short distance from ordinary albumen chamber. Spermoviduct (Figures 1C–F: **eo**) of ~1.5 whorl in length, slightly narrower than albumen gland, ~15 times longer than wide; extremely coiled and difficulty to untangle. Prostate gland occupying ~1/6 of spermoviduct surface and ~1/10 its volume (Figures 3D, E: **pt**). Uterus occupying most of spermoviduct space, external walls thick-glandular (Figures 3D, E: **ut**), inner surface completely covered with ample transverse chambers. Sperm groove simple, on posterior half of spermoviduct (Figure 3D: **sp**), on basal half becoming gradually protected by prominent fold (Figures 3E, 4B: **sp**); abruptly becoming tubular vas deferens on anterior end of spermoviduct (Figure 4B: **vd**). Free oviduct short (Figure 4B: **fo**), ~1/20 of spermoviduct length; inner surface with 4–5 wide longitudinal folds and wide groove running to bursa aperture. Vagina ~1/10 spermoviduct length (Figures 3C, 4B: **vg**); inner surface with same folds as free oviduct (Figure 4B: **vg**). Bursa copulatrix ~2/3 of spermoviduct length; bursa duct as wide as adjacent spermoviduct in its origin (Figure 3C: **bd**), gradually narrowing toward posterior end; bursa oval, ~1/8 of albumen gland size (Figure 3C: **bc**), encased between pericardium and adjacent intestinal loop. Penis ~1/2 of spermoviduct length, ~1/2 of spermoviduct anterior width (Figure 3C: **pe**); penis muscle inserting terminally, relatively short (Figures 3C, 4A: **pm**). Epiphallus ~1/8 penis length, located as short terminal continuation of penis (Figures 3C, 4A: **eh**), inner surface with narrow, regular longitudinal folds, located separated from each other, uniformly sized (Figure 4A: **eh**). Vas deferens inserted subterminally in penis tip (Figures 3C, 4A: **vd**). Internal penial surface lacking clear sub-chambers (Figure 4A: **pe**); except for inner loop located at middle level (Figure 4A: **po**) formed by penis' inner mucosa. Remaining inner penial surface with 4–5 inner, narrow, low, separated, longitudinal, uniform folds, all along surface, some of them converging to vas deferens aperture (Figure 4A: **vd**); except for ~1/4 of penial area anterior to loop, in which penial folds becoming longitudinal, branched furrows (Figure 4A). Penis shield occupying basal ~1/4 of penis length (Figures 3C, 4A: **ps**); vas deferens piercing its walls close to its base (Figure 4A). Genital pore round, simple. Genital muscle (Figures 3C, 4A: **gm**) located from genital aperture up to right secondary columellar muscle (Figure 2B: **gm**).

Central nervous system (Figure 4C): Well explored by La Pasta and Oliveira (2025: 371–372, figs. 18–19), except for more central ganglia. Cerebral commissure slightly narrower (~1/2 of each ganglion width) (**ce**). Both pleural ganglia (**pl**) separated from pair of pedal ganglia (pp) by wide slit in which thick vessel lies. Pair of pleural ganglia slightly smaller than cerebral ganglia. Pair of pedal ganglia ~1.5 times larger than cerebral ganglia.

Distribution: Still under analysis on whether it is widely distributed from NE Brazil up to Argentina, or if there are a set of similarly shelled species include within the nominal species. The analyzed material is from the Atlantic Rainforest in an area shared by Rio de Janeiro and São Paulo states, Brazil.

Habitat: Found living usually in shaded areas, on trunks and leaves of the tree vegetation of rainforests. But sometimes they are found in urban areas on walls and in gardens.

Measurements (length and width in mm): MZSP 90819: 32.6 by 13.4; MZSP 168356: 31.8 by 15.2; MZSP 158750: 31.8 by 13.7.

Material Examined: BRAZIL. São Paulo: Itariri, MZSP 90819, 10 specimens (A. Galdino col., 2009); Itanhaém (G. Alledo col.), 24°11'22" S 46°48'00" W, near road, MZSP 168356, 4 specimens (March 9, 2024), 24°10'54.48" S 46°47'06.12" W, MZSP 158750, 8 specimens (October 17, 2021).

DISCUSSION

The main distinctions between the continental *Drymaeus papyraceus*, based on populations from the coastal region of São Paulo, and *D. castilhensis*, *D. micropyrus*, and *D. currais*—three endemic insular species from islands off the São Paulo–Paraná coast—are summarized in Table 1. Several of these conchological and anatomical differences were already outlined in their original descriptions (Simone and Amaral, 2018; Simone et al., 2020) and were also noted by La Pasta and Oliveira (2025: 378–380). The present, more detailed investigation allows for a more in-depth assessment of the number and nature of differences among the four species.

The quantity and consistency of the phenotypic differences observed strongly indicate that each region harbors its own distinct species. It is important to emphasize that the set of characters presented is based on multiple specimens, all from the same area, which consistently share

Table 1. Differential diagnosis among the four *Drymaeus* species studied in this paper (abbreviations explained in text.)

Character	*D. currais*	*D. papyraceus*	*D. castilhensis*	*D. micropyrus*
Shell width/length	50%	40%	50%	48%
Spots color	Brown	Brown	Brown	Light beige
% spm lacking spots	10	0	20	0
Spire angle	55°	40°	50°	43°
% Protoc/length	6	4	6	4
Axial sculpture	Smooth	Strong	Smooth	Strong
Suture	Marked	Shallow	Marked	Marked
Peristome angle	20°	10°	20°	20°
Peristome length	50%	45%	50%	50%
Body whorl length	50%	65%	60%	50%
Columellar m length	1.8	1.6	1.5	1.5
Left (**lm**) origin	4	7	5	2
Right (**rm**) origin	2	4	6	4
Lm connect **cm**	Yes	Yes	No	No
Rm connect **cm**	Yes	No	Yes	Yes
Ureter ap (**ua**)	1/3	1/5	1/5	1/5
Ureter gutter (**ug**)	T with fold	T shaped simple	Y-shaped	Y-shaped
Pulmonary vessels in right of **cv**	entire	Only anterior 1/3	Only anterior 1/3	Mostly anterior 1/4
Od m1v	Medial	Lateral	Absent	Absent
Od m1d	Absent	Present	Absent	Absent
Od m2 insertions	2	6	2	2
Od m4 origins	Simple	Multiple	Simple	Simple
Od m5	Most covered by m4	½ exposed	Most covered by m4	Most covered by m4
Od m7	Absent	Medium	Posterior	Posterior
Od m10	Thin wide	Thick wide	Thin narrow	Thin narrow
Radular sac	Inlaid	Exposed	Exposed	Exposed
Ra rachidian size compared to neighb	~1/2	Almost same	~1/4	~1/3
Ra marginals # of outer second cusps	2	1	1	1
Ra # laterals	~55	~70	~25	~65
Jaw middle constriction	Present	Absent	Present	Absent
Salivary duct penetration	Esophagus origin	Close to sa	Esophagus origin	Esophagus origin
Salivary aperture	Middle	Lateral	Lateral	Lateral
Salivary aperture	Longitudinal	Opened pore	Transverse slit	Transverse slit
Stomach	Narrow	Bulged	Narrow	Narrow
Origin **dd**	Stomach	Esophagus	Intestine	Intestine
Origin **da**	Esophagus	Stomach	Stomach	Stomach
Insertion **hd** in **sr**	Base	Middle	Middle	Middle
Duct of **sr**	Long	Short	Short	Short

(*continued*)

Table 1. (Continued)

Character	*D. currais*	*D. papyraceus*	*D. castilhensis*	*D. micropyrus*
Genital appendix	Present	Absent	Absent	Absent
Albumen duct (**ad**)	Oblique, to eo	Perpedic, in sr	Double, inset to intersect eo-sr duct	Single, insert to intersect eo-sr duct
Albumen chamber (**ac**)	Sac + duct	Wide curve	Absent	Absent
Accessory albumen chamber (**ab**)	Present	Present	Present	Absent
Prostate width	¼	1/6	½	1/3
Heigh sp basal 1/3	Tall, thick, bifid	Tall, thin, simple	Tall, thick, simple	Low, thick, simple
Penis loop (**po**)	Absent	Present	Absent	Absent
Penis inner middle region	Smooth	With loop (po)	With inner middle glandular portion	With inner middle glandular portion
Genital muscle (**gm**)	Absent	present	Absent	Absent

this pattern and differ from those of other regions. Variable characters were excluded from the analysis.

Notable distinctions, particularly in shell morphology, radula, and the genital system—features traditionally regarded as especially informative—together with differences in other anatomical structures, suggest long-term genetic isolation and local adaptation. These patterns provide strong evidence that the examined taxa represent distinct entities. Some of these differences are discussed below; for illustrations and additional details, see the indicated references (Simone and Amaral, 2018; Simone et al., 2020).

With respect to the shell (Figures 1A–I), the continental *D. papyraceus* exhibits a more slender form, with a width-to-length ratio of approximately 40%, whereas the insular species show ratios of about 50%. It also presents a more strongly sculptured shell with a less deeply impressed suture, while the insular species generally have smoother shells (except for *D. micropyrus*, which shows slightly more pronounced axial undulations) and a deeper suture.

The spire is more acuminate in *D. papyraceus* and *D. micropyrus* (approximately 40°), whereas it is blunter in the other two species (approximately 52°). Additionally, the peristome is proportionally smaller in *D. papyraceus* (about 45% of shell length), while in the insular species it is closer to 50%.

The arrangement of the left and right secondary columellar muscles (Figure 2B: lm, rm) also differs among the four species (Table 1), particularly in the number of anterior insertions and in the presence or absence of a medial connection with the main columellar muscle (indicated as "rm" in Figure 2B). These features tend to be stable within populations.

The basal condition in bulimulids is for both the primary and secondary ureters to be closed (i.e., tubular). However, some species of *Drymaeus* constitute exceptions, exhibiting an anteriorly open ureter, as observed in the *D. papyraceus* group (Figure 2A: **ua**). Among these, *D. currais* shows the longest open portion (approximately 1/3 of the ureter length), whereas in the other three species the open portion is shorter (approximately 1/5).

Anterior to the open ureter, at the pneumostome, lies the urinary gutter, which is bifid in the *D. papyraceus* group (Figure 2A: **ug**). In *D. currais* and *D. papyraceus*, it is T-shaped, with *D. currais* further distinguished by the presence of a prominent satellite pallial fold. In *D. castilhensis* and *D. micropyrus*, the urinary gutter is Y-shaped and appears less developed.

The odontophore (Figures 2C, D; 3A) is broadly similar among these taxa, as is typical for closely related species. Nevertheless, some differences were observed in muscle pairs **m1**, **m2**, **m4**, and **m7** (Table 1). As discussed elsewhere (Simone, 2022b, 2025), odontophore muscles **m1** and **m7** tend to be the most variable at the species level, a pattern that is corroborated by the present study.

In contrast, muscles **m2** and **m4** are generally more conservative. However, in the present material, muscle m2 varies in the number of insertions (Table 1), whereas muscle **m4** shows variation in the shape of its origin.

The radula, a structure that is typically widely examined, exhibits relatively few differences among these species. Only the proportional size of the rachidian tooth and the number of cusps on the lateral teeth show some variation (Table 1).

The jaw plate, however, presents a notable distinction: *D. currais* and *D. castilhensis* exhibit a medial constriction, whereas *D. papyraceus* and *D. micropyrus* do not. Aside from this feature, the pattern of transverse ribs conforms to the typical condition observed in bulimulids.

The arrangement of the ducts to the digestive gland also differs among the four species (Table 1). The duct to the posterior lobe originates from the stomach in *D. currais*, from the esophagus in *D. papyraceus* (Figure 3B), and from the intestine in the remaining two species.

The duct to the anterior lobe arises from the esophagus in *D. currais*, at a relatively larger distance from the

stomach, whereas in the other three species it originates from the stomach.

In the genital system, the carrefour, or fertilization complex, is of particular interest due to its structural variation among species (Table 1). Figure 5 aids in the interpretation of these differences by presenting a schematic comparison (for detailed descriptions, see Simone and Amaral, 2018; Simone et al., 2020).

Drymaeus currais is the only species possessing a genital appendix (Figure 5A: **ga**). *Drymaeus papyraceus* is unique in having the albumen chamber represented as a curvature at the beginning of the spermoviduct (Figure 5B: ac), whereas *D. castilhensis* and *D. micropyrus* lack a distinct albumen chamber. In *D. castilhensis*, however, the duplicated duct of the albumen gland (Figure 5C: **ad**) may represent a vestigial chamber fused with the gland, a condition that appears to be more advanced in *D. micropyrus* (Figure 5D).

Drymaeus micropyrus, in turn, is the only species lacking an accessory albumen chamber (**ab**). In *D. currais*, the albumen chamber exhibits a more typical bulimulid condition (Figure 5A: **ac**), except that the albumen gland drains directly into the spermoviduct rather than into the chamber (Figure 5A: **ad**). This arrangement results in an elongated duct of the seminal receptacle (Figure 5A: **rd**), in contrast to the shorter condition observed in the other species.

The initial portion of the spermoviduct also differs among the four species. In *D. currais*, it begins at the junction of the albumen chamber duct and the duct of the seminal receptacle (Figure 5A: **ad–rd**). In *D. papyraceus*, it begins as a curved albumen chamber (Figure 5B: **ac**). In *D. castilhensis* and *D. micropyrus*, the spermoviduct effectively originates from the albumen chamber duct (Figures 5C, D: **ad**), with the duct of the seminal receptacle forming a lateral appendix (**rd**); *D. castilhensis* further differs in having duplicated ducts.

In the remaining regions of the genital system, additional distinctions are evident. The proportional width of the prostate, for example, varies among species (Table 1): it is very narrow in *D. papyraceus* (approximately 1/6 of the spermoviduct surface) (Figures 3D, E), broader in *D. castilhensis* (about 1/2), while the other two species exhibit intermediate proportions.

The fold protecting the sperm groove in the basal region of the spermoviduct (Figures 3E, 4B: **sp**) also differs structurally among species (Table 1). The penis is slender in all species, with an apical epiphallus. Its internal surface shows distinctive features in each species (Table 1), the most notable being the median loop observed in *D. papyraceus* (Figure 4A: **po**). This species is also unique in possessing a genital muscle (Figures 3C, 4B: **gm**) connected to the genital pore and originating from the right secondary columellar muscle (Figure 2B: **gm**), a condition commonly found in several stylommatophorans.

Interestingly, La Pasta and Oliveira (2025: 379–380) acknowledged the morphological differences among the four species but dismissed them as insufficient to support specific separation, instead proposing their synonymy. The differences they discussed were largely based on information from the original descriptive studies (Simone and Amaral, 2018; Simone et al., 2020), which at that time lacked anatomical data for *D. papyraceus*. The present study, by providing a more detailed anatomical account, adds a substantial set of additional differences. They also briefly discuss molecular CO1 distances among these species based on previous studies (Salvador et al., 2023; Rosa et al., 2025). They argue that the observed distances of 8–10% are insufficient to support species-level separation. However, when considered alongside the biogeographical and refined phenotypic data presented here, a different conclusion can be reached.

The quantity and consistency of both conchological and anatomical distinctions, together with their uniformity within each studied population, strongly indicate that these taxa represent distinct entities. Moreover, the three insular species are geographically isolated from the mainland by several dozen kilometers of ocean, constituting an effective barrier for terrestrial gastropods (Simone, 2022; Sparovek and Levkovicz, 2025). La Pasta and Oliveira (2025: 379), however, suggested that gene flow between these populations could occur via passive dispersal by birds, citing some studies (Schilthuizen and Lombaerts, 1994; Hausdorf and Hennig, 2003; Nekola, 2012). Such mechanisms, however, are generally considered exceptional and are invoked only when other explanations for isolation have been exhausted, which is not the case here.

They also proposed anthropogenic introduction as a possible explanation for the presence of *D. papyraceus* on these islands. However, this hypothesis is not supported by the absence of other well-known anthropogenically dispersed species in southeastern Brazil, which are typically transported more readily than native taxa, such as, e.g., *Bradybaena similaris* (Férussac, 1822), *Rumina decollata* (Linnaeus, 1758), *Subulina octona* (Bruguière, 1789), and *Lissachatina fulica* (Bowdich, 1822) (Simone, 2022a).

Furthermore, as discussed elsewhere (Simone, 2022a), present-day insular isolation may not be the primary factor underlying the differentiation of these species. The geographic isolation of southeastern Brazilian islands is relatively recent: it is well established that many of these islands were connected to the mainland until approximately 8,000 years ago (Vieira, 1981), when sea levels were about 120 m lower than at present, allowing for extensive forest continuity. This time span is likely insufficient for speciation to have occurred solely due to marine isolation. It is therefore plausible that the populations currently inhabiting these islands were already differentiated prior to insularization, with their isolation originally driven by other barriers, such as large rivers or estuarine systems.

The study of the central nervous system by La Pasta and Oliveira (2025: 372–373, figs. 18, 19), on the other hand, is noteworthy, extending well beyond the usual level of detail. They illustrated most of the central

nerves, representing a significant advance in the knowledge of this system. The central ganglia themselves, however, appear to remain somewhat unclear in that study.

This may be due to the thick layer of blood sinus tissue that typically envelops the nerve ring, which apparently was not removed, as suggested by the figures. For accurate observation, this tissue must be removed to expose only the nervous components; otherwise, the resulting image represents a mixture of neural and connective tissues, leading to misinterpretation. In the present study, a cleaned nerve ring is illustrated (Figure 4C), revealing a more slender cerebral commissure (**ce**) and a clear separation between the central regions of the pleural and pedal ganglia (**pl, pp**).

With regard to the nerve ring, La Pasta and Oliveira (2025: 279) stated that the insular *Drymaeus* species were described as lacking a cerebral commissure (Simone and Amaral, 2018; Simone et al., 2020). However, as the cerebral commissure is present in all Mollusca, it is typically mentioned only if discovered as absent or when it presents noteworthy features. Taxonomic descriptions generally emphasize relevant (diagnostic) characters and features that are shared within a broader taxonomic group are often omitted.

CONCLUSIONS

Given its wide distribution and regional variation, what is currently recognized as *Drymaeus papyraceus* likely represents a complex of morphologically similar species. The present study supports that.

At least the four populations examined in the present and previous studies clearly represent distinct taxa, as evidenced by the quantitative and qualitative differences in their conchological and morpho-anatomical characters (Table 1).

In closely related species, morpho-anatomical analyses must be both detailed and comprehensive in order to reveal taxonomically informative differences. Reliance on superficial knowledge on anatomy alone may lead to biased conclusions, as it is insufficient to demonstrate the necessary distinctions.

The three insular *Drymaeus* species are, thus, revalidated, as follows:

***Drymaeus castilhensis* Simone and Amaral,** 2018 (Figure 5C)

Drymaeus castilhensis Simone and Amaral, 2018: 168–179 (figs 2–9, 21–24, 37–54); Simone et al., 2020: 2, 3, 10; Simone, 2022a: 13 (fig. 2); Rosa *et al*., 2025: 2, 4, 5, 17–18; La Pasta and Oliveira, 2025: 368, 369, 378–390; MolluscaBase, 2026.

Diagnosis: Shell conical, width ~50% of length, aperture ample, weakly deflected. Color white-cream, mostly with strong dark brown axial spots; peri-umbilical area lacking spots; ~20% of specimens lacking spots. Spire angle ~50°. Protoconch ~6% of total length. Sculpture absent, smooth. Suture well-marked. Peristome profile angle ~20°; length ~60% of total length. Columellar muscle of 1.5 whorls. Secondary columellar muscles with 5 origins on left and 6 on right; only left connected to main columellar muscle. Secondary ureter almost entirely closed, except for ~1/5 of its length preceding pneumostome. Urinary gutter Y-shaped. Anus external to pneumostome, opened directly outside. Lung vessels more developed in anterior 1/3. Intrinsic pair of odontophore muscles: m1v absent, m1d absent, m2 with 2 insertions, m4 with simple insertions, m5 mostly covered by m4, m7 originating in cartilages close to m6, m10 thin and narrow. Sigmoid intestinal loop very ample. Radular sac exposed. Radular rachidian ~1/4 of neighboring teeth width; marginal teeth with 1 outer secondary cusp; ~25 lateral teeth. Jaw with middle constriction. Salivary duct penetrating in dorsal buccal mass wall close to esophageal origin. Aperture of salivary glands lateral in middle level of buccal cavity; as transverse slit. Stomach narrow, duct to posterior lobe of digestive gland originated from adjacent intestine; duct to anterior lobe originated from stomach. Seminal receptacle duct short. Genital carrefour appendix wanting. Albumen gland duct double, inserting in intersection between spermoviduct and seminal receptacle duct. Albumen chamber absent. Accessory albumen chamber present. Prostate occupying ~1/2 of spermoviduct surface; fold protecting sperm groove in inferior region inferior tall, thick and simple. Penis slender and long, lacking clear inner chambers; inner loop absent. Inner middle glandular portion in penis. Genital muscle absent. For the formal description see Simone and Amaral (2018).

Type Material: Holotype: MZSP 84277, several paratypes.

Type Locality: BRAZIL. **São Paulo State**: off Cananéia, Ilha de Castilho, 25°16'24.6" S 47°57'18.6" W.

***Drymaeus micropyrus* Simone and Amaral,** 2018 (Figure 5D)

Drymaeus micropyrus Simone and Amaral, 2018: 179–180 (figs. 10–14, 25–28, 53–55); Simone et al., 2020: 10; Simone, 2022a: 13 (fig. 2); 10; Rosa *et al*., 2025: 2, 17–18; La Pasta and Oliveira, 2025: 368, 369, 378–390; MolluscaBase, 2026.

Diagnosis: Shell conical, width ~48% of length, aperture ample, weakly deflected. Color greenish-cream, with brown narrow axial spots, joint forming larger axial spots; peri-umbilical area with same pigmentation. Spire angle ~43°. Protoconch ~4% of total length. Sculpture with axial undulations. Suture well-marked. Peristome profile angle ~20°; length ~50% of total length. Columellar muscle of 1.5 whorls. Secondary columellar muscles with 2 origins in left and 4 in right; only right connected to main

columellar muscle. Secondary ureter almost entirely closed, except for ~1/5 of its length preceding pneumostome. Urinary gutter Y-shaped. Anus external to pneumostome, opened directly outside. Lung vessels more developed in anterior 1/4. Intrinsic pair of odontophore muscles: m1v absent, m1d absent, m2 with 2 insertions, m4 with simple insertions, m5 mostly covered by m4, m7 originating in cartilages close to m6, m10 thin and narrow. Sigmoid intestinal loop very ample. Radular sac exposed. Radular rachidian ~1/3 of neighboring teeth width; marginal teeth with 1 outer secondary cusp; ~65 lateral teeth. Jaw lacking middle constriction. Salivary duct penetrating in dorsal buccal mass wall close to esophageal origin. Aperture of salivary glands lateral in middle level of buccal cavity; as transverse slit. Stomach narrow, duct to posterior lobe of digestive gland originated from adjacent intestine; duct to anterior lobe originated from stomach. Seminal receptacle duct short. Genital carrefour appendix wanting. Albumen gland duct single, giving origin to spermoviduct, seminal receptacle duct connected in a side. Albumen chamber absent. Accessory albumen chamber absent. Prostate occupying ~1/3 of spermoviduct surface; fold protecting sperm groove in inferior region inferior low, thick and simple. Penis slender and long, lacking clear inner chambers; inner loop absent. Inner middle glandular portion in penis. Genital muscle absent. For the formal description see Simone and Amaral (2018).

Type Material: Holotype: MZSP 84939. Some non-type material.

Type Locality: BRAZIL. **São Paulo State**; off Peruíbe, Ilha Queimada Pequena (Queimadinha) 24°22'31" S, 46°48'24" W.

Drymaeus currais Simone, Belz and Gernet, 2020 (Figure 5A)

Drymaeus currais Simone et al., 2020: 2–10 (figs. 1–36); Simone, 2022a: 13 (fig. 2); Rosa *et al.*, 2022: 6; Rosa *et al*., 2025: 2, 17–18; La Pasta and Oliveira, 2025: 368, 369, 378–390; MolluscaBase, 2026.

Diagnosis: Shell conical, width ~50% of length, aperture ample, weakly deflected. Color white-cream, mostly with strong axial, dark brown spots; peri-umbilical area lacking spots; ~10% of specimens lacking spots. Spire angle ~55°. Protoconch ~6% of total length. Sculpture absent, smooth. Suture well-marked. Peristome profile angle ~20°; length ~50% of total length. Columellar muscle of 1.8 whorls. Secondary columellar muscles with 4 origins in left and 2 in right; both muscles connected to main columellar muscle. Secondary ureter almost entirely closed, except for ~1/3 of its length preceding pneumostome. Urinary gutter T-shaped, possessing large fold. Anus external to pneumostome, opened directly outside. Lung vessels developed entirely along right side of pulmonary vein. Intrinsic pair of odontophore muscles: m1v medial located, m1d absent, m2 with 2 insertions, m4 with simple insertions, m5 mostly covered by m4, m7 absent, m10 thin and wide. Sigmoid intestinal loop very ample. Radular sac inlaid inside buccal mass. Radular rachidian ~1/2 of neighboring teeth width; marginal teeth with 2 outer secondary cusp; ~55 lateral teeth. Jaw with middle constriction. Salivary duct penetrating in dorsal buccal mass wall close to esophageal origin. Aperture of salivary glands medial in middle level of buccal cavity; as longitudinal slit. Stomach narrow, duct to posterior lobe of digestive gland originated from stomach; duct to anterior lobe originated from adjacent esophagus. Seminal receptacle duct long. Genital carrefour appendix present. Albumen chamber duct single, giving origin to spermoviduct buy side of duct of receptacle. Albumen chamber sac-like, with its proper duct. Accessory albumen chamber present. Prostate occupying ~1/4 of spermoviduct surface; fold protecting sperm groove in inferior region inferior tall, thick and bifid. Penis slender and long, lacking clear inner chambers; inner loop absent. Inner middle smooth portion in penis. Genital muscle absent. For the formal description see Simone and Amaral (2018).

Type Material: Holotype: MZSP 150548, several paratypes.

Type Locality: BRAZIL. **Paraná State:** Off Pontal do Paraná, Currais Archipelago, Guapirá Island, 25°44'09.32" S, 48°21'55.34" W.

ACKNOWLEDGMENTS

I am especially grateful to Jon Ablett, the editor, and one anonymous reviewer for their comments and improvements to the manuscript. This paper was also previously shared with both authors of the article that prompted the present discussion. Dr. Cléo Oliveira replied, indicating that he was pleased with the fine-tuning of the taxonomy of the species discussed herein.

LITERATURE CITED

Castelló, J. R. 2020. Felids and hyenas of the World: wildcats, panthers, lynx, pumas, ocelots, caracals, and relatives. Princeton Field Guides, 572 pp.

Hausdorf, B. and C. Hennig. 2003. Nestedness of north-west European land snail ranges as a consequence of differential immigration from Pleistocene glacial refuges. Oecologia 135 (1): 102–109.

La Pasta, A. L. and C. D. C. Oliveira, 2025. Reassessment of two species from taxonomically inflated genera: *Drymaeus* Albers, 1850 and *Antidrymaeus* Germain, 1907 (Gastropoda: Bulimulidae). The Nautilus 139 (4): 367–383.

MolluscaBase eds. 2026. MolluscaBase. Accessed at: https://www.molluscabase.org/aphia.php?p=taxdetails&id=1308285 on 2026-03-15.

Nekola, J. C. 2012. The impact of a utility corridor on terrestrial gastropod biodiversity. Biodiversity and Conservation 21 (3): 781–795.

Rosa, R. M., D. C. Cavallari, and R. B. Salvador. 2022. iNaturalist as a tool in the study of tropical molluscs. PLoS One 17 (5): e0268048.

Rosa, R. M., R. B. Salvador, and D. C. Cavallari. 2025. The disappearing act of the magician tree snail: anatomy, distribution, and phylogenetic relationships of *Drymaeus magus* (Gastropoda: Bulimulidae), a long-lost species hidden in plain sight. Zoological Journal of the Linnean Society 203 (3): zlaf017.

Salvador, R. B., F. S. Silva, D. C. Cavallari, F. Kohler, J. Slapcinsky, and A. S. H. Breure. 2023. Molecular phylogeny of the Orthalicoidea land snails: Further support and surprises. PLoS One 18 (7): e0288533. doi: 10.1371/journal.pone.0288533.

Schilthuizen, M. and M. Lombaerts. 1994. Population structure and levels of gene flow in the mediterranean land snail *Albinaria corrugata* (Pulmonata: Clausiliidae). Evolution 48 (3): 577–586.

Simone, L. R. L., 2007. Estudos de morfologia detalhada e de filogenia em moluscos: uma análise comparativa. Tópicos em Malacologia – Ecos do XVIII EBRAM. Sociedade Brasileira de Malacologia. Rio de Janeiro, 189–201. páginas iniciais - ok

Simone, L. R. L., 2022a. Islands: an important source of mollusk endemicity. Malacopedia 5 (2): 11–16. https://www.moluscos.org/trabalhos/Malacopedia/05-02Malacopedia-Islands.pdf

Simone, L. R. L., 2022b. The molluscan jugal muscles – m1. Malacopedia 5 (5): 43–48. https://moluscos.org/trabalhos/Malacopedia/05-05Simone%202022%20Malacopedia-jugal%20muscle%20m1.pdf

Simone, L. R. L., 2025. The radular sac muscles – m7. Malacopedia 8 (7): 44–52. https://moluscos.org/trabalhos/Malacopedia/08-07Simone%202025%20m7.pdf

Simone, L. R. L. and V. S. Amaral. 2018. Insular live: new endemic species from São Paulo oceanic islands, Brazil (Pulmonata, Bulimulidae), as example of endemicity. Journal of Conchology 43 (2): 167–187.

Simone, L. R. L., C. E. Belz, and M. V. Gernet. 2020. A new species of *Drymaeus* endemic from Currais Archipelago, Paraná, Brazil (Pulmonata, Bulimulidae). Papéis Avulsos de Zoologia 60: e20206057, https://doi.org/10.11606/1807-0205/2020.60.57.

Sparovek, G. and Levkovicz, R. 2025. Área de proteção ambiental marinha Litoral Sul – Diagnóstico. Versão Executiva. Fundação Florestal. São Paulo, 188 pp.

Vieira, P. C. 1981. Variações do nível marinho: alterações eustáticas no Quaternário. Revista do Instituto Geológico 2 (1): 39–58.